High-Performance Silicon Optoelectronic Devices Based on Graphene

Subjects: Optics
Contributor: Siqi Yan

Graphene—a two-dimensional allotrope of carbon in a single-layer honeycomb lattice nanostructure—has several distinctive optoelectronic properties that are highly desirable in advanced optical communication systems. Meanwhile, silicon photonics is a promising solution for the next-generation integrated photonics, owing to its low cost, low propagation loss and compatibility with CMOS fabrication processes.

graphene silicon photonics optics communications

1. Introduction

The ongoing fourth industrial revolution [1] is driven by the tremendous quantities of data associated with the internet of things [2], cloud computing [3], and big data analytics [4]. Fast and highly efficient tele- and data-communication systems are essential to support these data intensive technologies. Optical communication technology plays a key role in nearly every aspect of the modern communication links such as access networks, aggregation networks and core networks [5]. Silicon optical interconnect chips, especially silicon modulators and photodetectors, are at the heart of communication networks, thanks to their CMOS compatible fabrication process, cost- and energy-efficient properties [6][7][8].

2. Physical Properties and Hybrid Graphene/Silicon Fabrication Processes

Graphene, a single-atomic-layer system consisting solely of carbon atoms formed in a hexagonal lattice, holds several distinctive physical properties owing to its unique linear energy dispersion relation [9]. These properties make it an ideal enhancement towards the silicon modulators and detectors. Among these properties, the ultrahigh carrier mobility of graphene is most widely exploited since it enables the ultrafast silicon modulator and photodetector [10][11][12][13]. Moreover, thanks to the gapless nature of graphene, it absorbs photons in wavelengths ranging from the visible to the infrared. This is highly favorable for photodetection operating in the telecommunications C-band (1530–1565 nm), in which silicon is transparent. Furthermore, graphene’s extraordinarily large heat conductivity and relatively low light absorption can be exploited in high-performance nanoscale thermos-optic phase shifters within silicon photonics. These properties combine to exhibit superior performance in terms of the tuning efficiency and response time [14][15][16][17][18], when compared to traditional p-i-n or metallic microheater structures.

The fabrication process of the silicon/graphene hybrid devices typically consists of three steps. The first step is the fabrication of passive silicon photonic circuit. In this step, the grating coupler, waveguides, and other passive elements is fabricated using a lithographic and etching processes. Subsequent planarization then allows the graphene to be placed flat on top of the silicon structures. Generally, graphene is first deposited with a chemical vapor deposition (CVD) process on a cooper coil. Then, it is then transferred onto the target area of the chip using a wet or dry transfer process [19]. This step is crucial, and the most challenging, as the quality of the transfer (and therefore of the graphene sample on the device) determines the performance of the graphene-based components on the chip. The third step is the patternization and metallization of the silicon/graphene hybrid chip, which is achieved by standard CMOS fabrication processes. In order to reach ideal Ohmic contact between the graphene and the metal pad, the type of the metal should be carefully chosen since large contact resistance can lead to large *RC* constant thus low operation speed of the device. Normally, titanium (Ti), palladium (Pd) and platinum (Pt) are ideal choices since they hold low contact resistance with graphene [20].

3. High-Performance Modulation Devices Based on Graphene

In optical telecommunications scenarios, optical modulators are used to convert the encoding of electronic data to the optical domain. Any combination of photonic degrees of freedom can be utilized, for example intensity, phase, and/or frequency [21][22][23]. Afterwards low-loss optical fibers are used to achieve long distance communication links. Integrated silicon optical modulators allow an orders-of-magnitude decrease in size, weight and power in modulation systems, and thus have attracted great attention since their first demonstrations [23].

Among these modulation mechanisms, intensity modulation is most widely applied due to its simplicity. There are two typical methods to realize intensity modulation in integrated silicon chips. One method is to directly alter the absorption of the active medium, and the other is to convert phase modulation to intensity modulation with interference structures, for example using a Mach-Zehnder interferometer (MZI) or a micro-ring resonator (MRR). Both methods rely on the efficient modulation of either the refractive index of the waveguide or the absorption of the active medium. For both types of phase shifter, graphene’s impressive optical and electrical properties offer a significant enhancement in key performance metrics, such as bandwidth and power consumption.

4. High-Performance Photodetector Based on Graphene

Due to its transparency in the telecommunications C-band near 1550 nm, silicon is inefficient in converting light into an electrical signal. Up to now, the mainstream of integrated photodetectors in silicon photonics for the communication wavelengths includes employing germanium (Ge) or monolayer graphene as photodetection material [24][25]. Ge-Si hybrid photodetectors have been widely studied and reached significant maturity thanks to their ability to absorb light in the telecommunications band near 1550 nm. High responsivity larger than 1 A/W has been achieved and an impressive bandwidth of 265 GHz has been demonstrated recently [24][26]. Compared to Ge/Si photodetectors, graphene/Si photodetectors hold great potential in reaching ultra large operation bandwidth thanks to the ultrahigh carrier mobility of graphene as well as its absorption ability in a broader wavelength range. For graphene/silicon photodetectors, there are three different mechanisms for the photodetection, which are photovoltaic effect (PV), photo-thermoelectric effect (PTE) and photo-bolometric effect (PB). The graphene photodetectors based on these three mechanisms are discussed in detail below.

The PV effect relies on the separation of photoexcited electrons and holes by an applied electric field to generate photocurrent, which can be utilized by graphene/silicon photodetector structures with normal light incidence [24][25]. As the representative work of early endeavors in graphene-based photodetectors, Xia et al. demonstrated that the graphene/Si photodetectors can reach 40 GHz [26]. Moreover, the intrinsic response time of graphene photodetectors is experimentally demonstrated to be 2.1 ps, indicating a high bandwidth of 262 GHz (**Figure 1**a) [27].

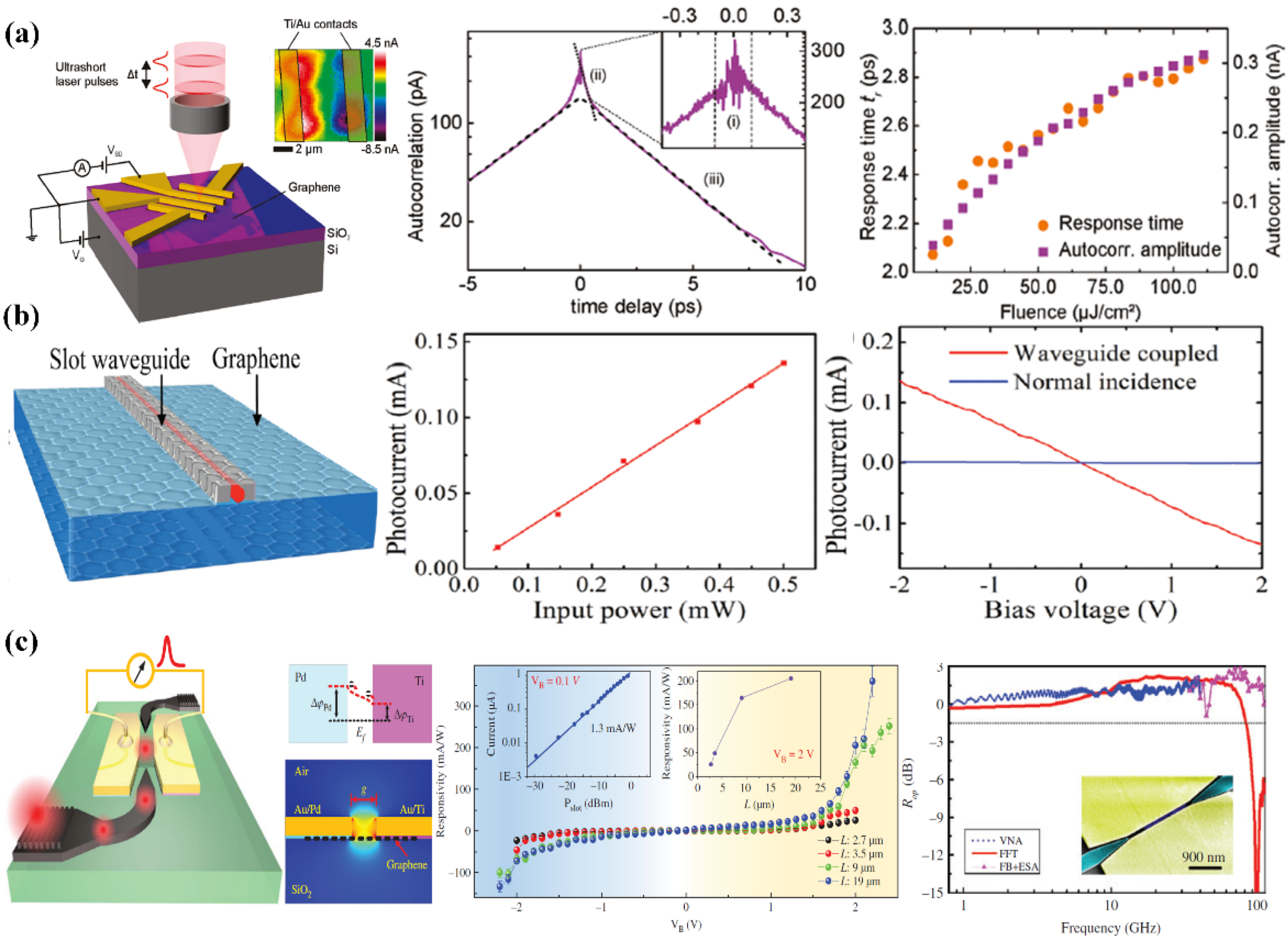

Figure 1. Graphene/silicon photodetector based on PV effect. (**a**) First graphene photodetector operating at 1550 nm. Reprinted with permission from *Nano Lett.* 2011, 11, 7, 2804–2808. Copyright 2011 American Chemical Society. (**b**) The graphene photodetector based on the silicon slot waveguide. Reproduced from Ref. [28] with permission from the Royal Society of Chemistry [27]. (**c**) The plasmonic enhanced high-performance graphene photodetector [29].

However, the responsivities of graphene-based photodetectors with normal light incidence are normally low. To increase the light-graphene interaction and obtain better performances, waveguide-based photodetectors have been extensively researched [11][30][29][31][32]. A typical waveguide integrated structure is shown in **Figure 1**b [30]. In their design, the graphene lies on top of the silicon slot waveguide as the absorption layer. Here, the graphene monolayer absorbs the light within the waveguide mode's evanescent field, and a responsivity of 0.273 A/W is measured.

Meanwhile, hybrid integration of the silicon waveguide and graphene could also be fabricated at the wafer-scale, thanks to its low fabrication complexity [33]. The proposed photodetector holds a bandwidth of 41 GHz and the maximum responsivity is 46 mA/W. To further optimize the performance of the photodetector, Ding et al. proposed a waveguide-coupled integrated graphene plasmonic photodetector (**Figure 1**c) [29]. The plasmonic slot waveguide is formed by two different metallic slabs with a gap of 120 nm. This structure induces subwavelength light confinement within the surface of the graphene, dramatically increasing light absorption within the graphene. Meanwhile, different types of metal cause different doping levels in the graphene, enhancing the internal electrical field in the gap and more effectively separating the photogenerated carriers, leading to a high responsivity. Owing to these two points, the device features responsivity up to 0.36 A/W and an operation bandwidth larger than 110 GHz.

When the plasmonic gap becomes even narrower (less than 50 nm), there exist a competition between the PV and PB effect within the photodetection process, as Ma et al. thoroughly investigated [34]. An impressively high responsivity of 0.7 A/W at 1310 nm is achieved based on their work with PB effect. The PB effect refers to the modification of the channel resistance by either a change in the number of carriers or a change of the temperature-dependent carrier mobility. Thus, the PB effect leads to a negative photocurrent due to the increased channel resistance caused by the smaller mean free path induced by a temperature change due to photon absorption. A typical work based on PB effect is reported by Ma Ping employing a bowtie structure to reach a high responsivity of 0.5 A/W and a bandwidth of 110 GHz (**Figure 2**a) [35]. Wang et al. demonstrated a coherent, plasmonic-structure-based graphene optical receiver (**Figure 2**b) which is capable of the reception of both a 200 Gbit/s quadrature phase-shift keying (QPSK) signal and a 240 Gbit/s 16 quadrature amplitude modulation (16 QAM) signal on a single-polarization carrier, thanks to the ultrahigh operation bandwidth of the graphene photodetector [31]. Finally, a plasmonic/silicon hybrid graphene photodetector covering 1.55 μm and 2 μm is reported by Guo et al. where the responsivity is 0.07 A/W and 0.4 A/W at 1.55 μm and 2 μm respectively [36].

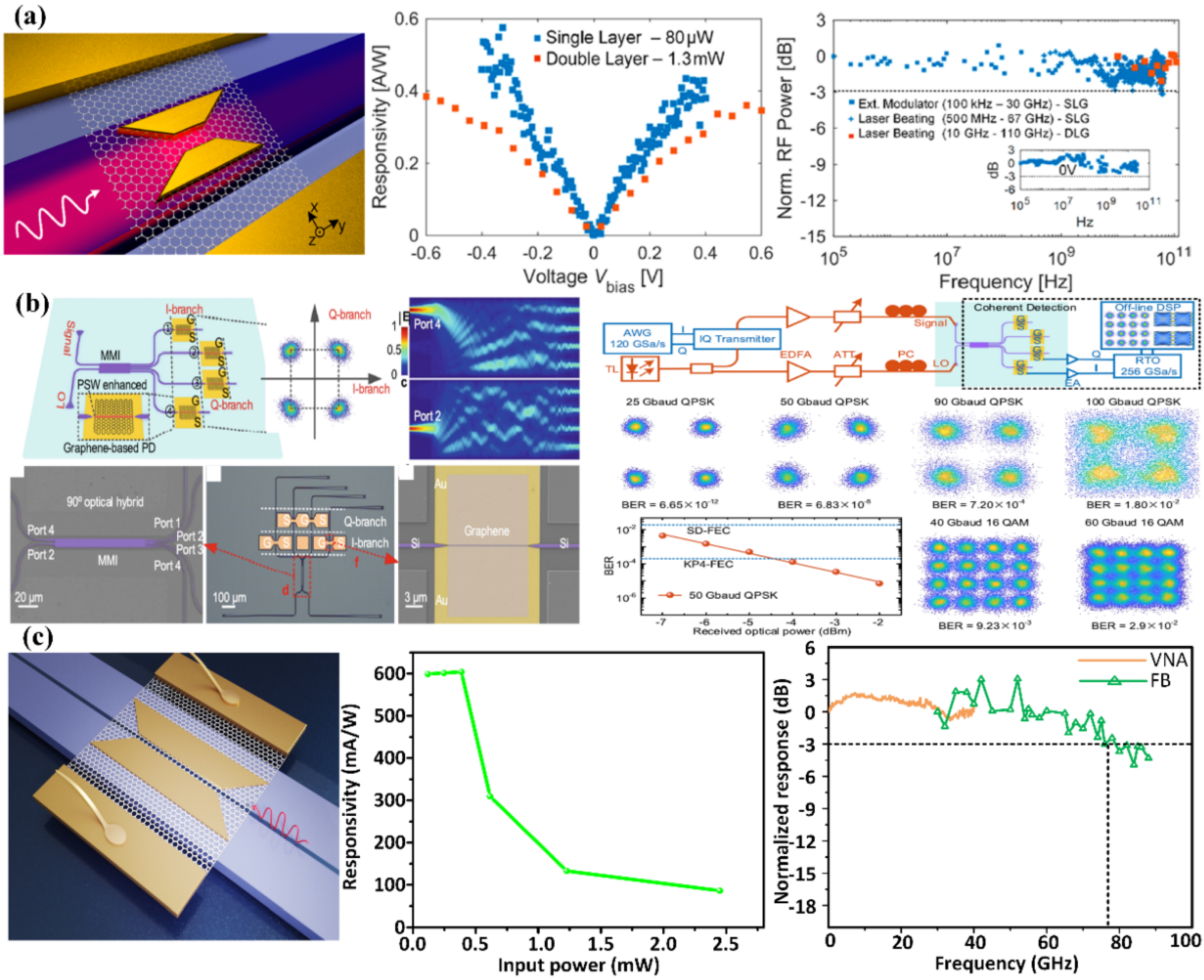

Figure 2. Graphene/silicon photodetectors based on PB effect. (**a**) Plasmonic enhanced graphene photodetector based on bowtie structure. Reprinted with permission from *ACS Photonics* 2019, 6, 1, 154–161. Copyright 2019 American Chemical Society. (**b**) Coherent optical receiver based on four graphene photodetectors [31]. (**c**) Double-slot graphene photodetector with a high responsivity [32].

From the above-mentioned works on plasmonic graphene photodetectors, we can conclude that plasmonic structures can dramatically optimize both the responsivity and the bandwidth of graphene-based receivers. Metallic absorption remains an obstacle, acting to reduce responsivity, since its characteristic absorption does not contribute to the photocurrent. To address this issue, Yan et al. proposed and demonstrated a double slot structure consisting of both the silicon slot waveguide and the plasmonic slot waveguide (**Figure 2**c) [32]. By optimizing the structural parameters, the metallic absorption is reduced to 0.2 dB/μm and the responsivity increased to 0.6 A/W.

Besides the PV and PB effect, the PTE effect has also recently been employed in silicon/graphene photodetectors. The PTE effect uses on the photon-induced electron temperature difference between two different graphene doping regions, which is normally achieved by external gating. Thus, the photocurrent is generated by an optically induced temperature gradient, which is proportional to the Seebeck coefficient. By optimizing the gate and source voltages simultaneously, a maximum responsivity of 0.36 A/W and a 3-dB operation bandwidth of 42 GHz is reached [37].

Moreover, photodetectors based on PTE effect can directly convert the optical signal to voltage signal, removing the need for a transimpedance amplifier. Various structures including photonic crystal waveguides [38], mircro-ring resonators [39] and double layer graphene [40] have been employed to enhance the light-matter interaction of the PTE effect, reaching impressive performances, such as responsivity higher than 90 V/W and operation bandwidths larger than 65 GHz. Although the external gating function adds complexity to the fabrication process compared to the photodetectors based on PV and PB effect, the PTE graphene photodetector is appealing to industry since it supports the direct connection between the photodetector and the read-out electric circuit. The performances of a typical graphene/silicon photodetector and state-of-the-art photodetectors based on conventional bulk materials is compared in **Table 1**. Graphene/silicon photodetector can achieve high ultra-high bandwidth more than 110 GHz, thanks to the ultrahigh carrier mobility of graphene. The responsivity of graphene photodetector is comparable with the other material platforms and can be further improved with further optimization by enhancing the light-graphene overlap and interaction.

Table 1. Comparison of the key parameters of the state-of-the-art photodetectors based on different materials.

Absorption Material	Responsivity	Bandwidth	Size	Operation Wavelength Range
InGaAs [41]	0.68 A/W	32 GHz	1 μm	1260 nm~1360 nm
InP [42]	0.8 A/W	40 GHz	5 μm	1240 nm~1650 nm
InP [43]	0.5 A/W	130 GHz	N. A.	1310 nm and 1550 nm
α-Ge [44]	0.35 A/W	>100 GHz	20 μm	1270 nm~1330 nm
Ge [26]	0.3 A/W	265 GHz	10 μm	1550 nm
Graphene [29]	0.36 A/W	>110 GHz	20 μm	1540 nm
Graphene [32]	0.6 A/W	78 GHz	30 μm	1550 nm

Absorption Material	Responsivity	Bandwidth	Size	Operation Wavelength Range
Graphene [35]	0.5 A/W	>110 GHz	6 μm	1480 nm~1620 nm
Graphene [36]	0.4 A/W	>40 GHz	20 μm	1550 nm and 2000 nm

1. Xu, M.; David, J.M.; Kim, S.H. The fourth industrial revolution: Opportunities and challenges. Int. J. Financ. Res. 2018, 9, 90–95.
2. Ashton, K. That ‘Internet of Things’ thing. RFID J. 2009, 22, 97–114.
3. Wang, L.; Von Laszewski, G.; Younge, A.; He, X.; Kunze, M.; Tao, J.; Fu, C. Cloud computing: A perspective study. New Gener. Comput. 2010, 28, 137–146.
4. Tsai, C.-W.; Lai, C.-F.; Chao, H.-C.; Vasilakos, A.V. Big data analytics: A survey. J. Big Data 2015, 2, 21.
5. Miller, S. Optical Fiber Telecommunications; Elsevier: Amsterdam, The Netherlands, 2012.
6. Jalali, B.; Fathpour, S. Silicon photonics. J. Lightwave Technol. 2006, 24, 4600–4615.
7. Soref, R. The past, present, and future of silicon photonics. IEEE J. Sel. Top. Quantum Electron. 2006, 12, 1678–1687.
8. Thomson, D.; Zilkie, A.; Bowers, J.E.; Komljenovic, T.; Reed, G.T.; Vivien, L.; Marris-Morini, D.; Cassan, E.; Virot, L.; Fédéli, J.-M. Roadmap on silicon photonics. J. Opt. 2016, 18, 073003.
9. Novoselov, K.S.; Geim, A.K.; Morozov, S.V.; Jiang, D.; Katsnelson, M.I.; Grigorieva, I.V.; Dubonos, S.V.; Firsov, A.A. Two-dimensional gas of massless Dirac fermions in graphene. Nature 2005, 438, 197–200.
10. Ponomarenko, L.A.; Yang, R.; Mohiuddin, T.M.; Katsnelson, M.I.; Novoselov, K.S.; Morozov, S.V.; Zhukov, A.A.; Schedin, F.; Hill, E.W.; Geim, A.K. Effect of a high-κ environment on charge carrier mobility in graphene. Phys. Rev. Lett. 2009, 102, 206603.
11. Gan, X.; Shiue, R.-J.; Gao, Y.; Meric, I.; Heinz, T.F.; Shepard, K.; Hone, J.; Assefa, S.; Englund, D. Chip-integrated ultrafast graphene photodetector with high responsivity. Nat. Photonics 2013, 7, 883–887.
12. Phare, C.T.; Daniel Lee, Y.-H.; Cardenas, J.; Lipson, M. Graphene electro-optic modulator with 30 GHz bandwidth. Nat. Photonics 2015, 9, 511–514.
13. Agarwal, H.; Terrés, B.; Orsini, L.; Montanaro, A.; Sorianello, V.; Pantouvaki, M.; Watanabe, K.; Taniguchi, T.; van Thourhout, D.; Romagnoli, M.; et al. 2D-3D integration of hexagonal boron

nitride and a high-κ dielectric for ultrafast graphene-based electro-absorption modulators. Nat. Commun. 2021, 12, 1070.

14. Yu, L.; Dai, D.; He, S. Graphene-based transparent flexible heat conductor for thermally tuning nanophotonic integrated devices. Appl. Phys. Lett. 2014, 105, 251104.
15. Gan, S.; Cheng, C.; Zhan, Y.; Huang, B.; Gan, X.; Li, S.; Lin, S.; Li, X.; Zhao, J.; Chen, H.; et al. A highly efficient thermo-optic microring modulator assisted by graphene. Nanoscale 2015, 7, 20249–20255.
16. Schall, D.; Mohsin, M.; Sagade, A.A.; Otto, M.; Chmielak, B.; Suckow, S.; Giesecke, A.L.; Neumaier, D.; Kurz, H. Infrared transparent graphene heater for silicon photonic integrated circuits. Opt. Express 2016, 24, 7871–7878.
17. Yu, L.; Yin, Y.; Shi, Y.; Dai, D.; He, S. Thermally tunable silicon photonic microdisk resonator with transparent graphene nanoheaters. Optica 2016, 3, 159–166.
18. Xu, Z.; Qiu, C.; Yang, Y.; Zhu, Q.; Jiang, X.; Zhang, Y.; Gao, W.; Su, Y. Ultra-compact tunable silicon nanobeam cavity with an energy-efficient graphene micro-heater. Opt. Express 2017, 25, 19479–19486.
19. Suk, J.W.; Kitt, A.; Magnuson, C.W.; Hao, Y.; Ahmed, S.; An, J.; Swan, A.K.; Goldberg, B.B.; Ruoff, R.S. Transfer of CVD-Grown Monolayer Graphene onto Arbitrary Substrates. ACS Nano 2011, 5, 6916–6924.
20. Matsuda, Y.; Deng, W.-Q.; Goddard, W.A. Contact Resistance for “End-Contacted” Metal−Graphene and Metal−Nanotube Interfaces from Quantum Mechanics. J. Phys. Chem. C 2010, 114, 17845–17850.
21. Reed, G.T.; Mashanovich, G.; Gardes, F.Y.; Thomson, D.J. Silicon optical modulators. Nat. Photonics 2010, 4, 518–526.
22. Almeida, V.R.; Barrios, C.A.; Panepucci, R.R.; Lipson, M. All-optical control of light on a silicon chip. Nature 2004, 431, 1081–1084.
23. Xu, Q.; Schmidt, B.; Pradhan, S.; Lipson, M. Micrometre-scale silicon electro-optic modulator. Nature 2005, 435, 325–327.
24. Benedikovic, D.; Virot, L.; Aubin, G.; Amar, F.; Szelag, B.; Karakus, B.; Hartmann, J.-M.; Alonso-Ramos, C.; Roux, X.L.; Crozat, P.; et al. 25 Gbps low-voltage hetero-structured silicon-germanium waveguide pin photodetectors for monolithic on-chip nanophotonic architectures. Photonics Res. 2019, 7, 437–444.
25. Benedikovic, D.; Virot, L.; Aubin, G.; Hartmann, J.-M.; Amar, F.; Le Roux, X.; Alonso-Ramos, C.; Cassan, E.; Marris-Morini, D.; Crozat, P.; et al. 40 Gbps heterostructure germanium avalanche photo receiver on a silicon chip. Optica 2020, 7, 775–783.

26. Lischke, S.; Peczek, A.; Morgan, J.S.; Sun, K.; Steckler, D.; Yamamoto, Y.; Korndörfer, F.; Mai, C.; Marschmeyer, S.; Fraschke, M.; et al. Ultra-fast germanium photodiode with 3-dB bandwidth of 265 GHz. Nat. Photonics 2021, 15, 925–931.
27. Wang, J.; Cheng, Z.; Chen, Z.; Wan, X.; Zhu, B.; Tsang, H.K.; Shu, C.; Xu, J. High-responsivity graphene-on-silicon slot waveguide photodetectors. Nanoscale 2016, 8, 13206–13211.
28. Luan, C.; Liu, Y.; Ding, Y.; Hu, H. 2-um high-speed graphene electro-optic modulator based on silicon slot microring resonator. In Proceedings of the Conference on Lasers and Electro-Optics, Washington, DC, USA, 10–15 May 2020; p. JTh2F.34.
29. Ding, Y.; Cheng, Z.; Zhu, X.; Yvind, K.; Dong, J.; Galili, M.; Hu, H.; Mortensen, N.A.; Xiao, S.; Oxenløwe, L.K. Ultra-compact integrated graphene plasmonic photodetector with bandwidth above 110 GHz. Nanophotonics 2020, 9, 317–325.
30. Shu, H.; Su, Z.; Huang, L.; Wu, Z.; Wang, X.; Zhang, Z.; Zhou, Z. Significantly High Modulation Efficiency of Compact Graphene Modulator Based on Silicon Waveguide. Sci. Rep. 2018, 8, 991.
31. Wang, Y.; Li, X.; Jiang, Z.; Tong, L.; Deng, W.; Gao, X.; Huang, X.; Zhou, H.; Yu, Y.; Ye, L.; et al. Ultrahigh-speed graphene-based optical coherent receiver. Nat. Commun. 2021, 12, 5076.
32. Yan, S.; Zuo, Y.; Xiao, S.; Oxenløwe, L.K.; Ding, Y. High-performance Silicon/Graphene Photodetector Employing Double Slot Structure. In Proceedings of the Conference on Lasers and Electro-Optics, San Jose, CA, USA, 9–14 May 2021; p. STh5B.2.
33. Schall, D.; Neumaier, D.; Mohsin, M.; Chmielak, B.; Bolten, J.; Porschatis, C.; Prinzen, A.; Matheisen, C.; Kuebart, W.; Junginger, B.; et al. 50 GBit/s Photodetectors Based on Wafer-Scale Graphene for Integrated Silicon Photonic Communication Systems. ACS Photonics 2014, 1, 781–784.
34. Ma, Z.; Kikunaga, K.; Wang, H.; Sun, S.; Amin, R.; Maiti, R.; Tahersima, M.H.; Dalir, H.; Miscuglio, M.; Sorger, V.J. Compact Graphene Plasmonic Slot Photodetector on Silicon-on-Insulator with High Responsivity. ACS Photonics 2020, 7, 932–940.
35. Ma, P.; Salamin, Y.; Baeuerle, B.; Josten, A.; Heni, W.; Emboras, A.; Leuthold, J. Plasmonically Enhanced Graphene Photodetector Featuring 100 Gbit/s Data Reception, High Responsivity, and Compact Size. ACS Photonics 2019, 6, 154–161.
36. Guo, J.; Li, J.; Liu, C.; Yin, Y.; Wang, W.; Ni, Z.; Fu, Z.; Yu, H.; Xu, Y.; Shi, Y.; et al. High-performance silicon−graphene hybrid plasmonic waveguide photodetectors beyond 1.55 μm. Light Sci. Appl. 2020, 9, 29.
37. Shiue, R.-J.; Gao, Y.; Wang, Y.; Peng, C.; Robertson, A.D.; Efetov, D.K.; Assefa, S.; Koppens, F.H.L.; Hone, J.; Englund, D. High-Responsivity Graphene–Boron Nitride Photodetector and Autocorrelator in a Silicon Photonic Integrated Circuit. Nano Lett. 2015, 15, 7288–7293.

38. Schuler, S.; Schall, D.; Neumaier, D.; Schwarz, B.; Watanabe, K.; Taniguchi, T.; Mueller, T. Graphene Photodetector Integrated on a Photonic Crystal Defect Waveguide. ACS Photonics 2018, 5, 4758–4763.

39. Schuler, S.; Muench, J.E.; Ruocco, A.; Balci, O.; van Thourhout, D.; Sorianello, V.; Romagnoli, M.; Watanabe, K.; Taniguchi, T.; Goykhman, I.; et al. High-responsivity graphene photodetectors integrated on silicon microring resonators. Nat. Commun. 2021, 12, 3733.

40. Mišeikis, V.; Marconi, S.; Giambra, M.A.; Montanaro, A.; Martini, L.; Fabbri, F.; Pezzini, S.; Piccinini, G.; Forti, S.; Terrés, B.; et al. Ultrafast, Zero-Bias, Graphene Photodetectors with Polymeric Gate Dielectric on Passive Photonic Waveguides. ACS Nano 2020, 14, 11190–11204.

41. Mauthe, S.; Baumgartner, Y.; Sousa, M.; Ding, Q.; Rossell, M.D.; Schenk, A.; Czornomaz, L.; Moselund, K.E. High-speed III-V nanowire photodetector monolithically integrated on Si. Nat. Commun. 2020, 11, 4565.

42. Xue, Y.; Han, Y.; Tong, Y.; Yan, Z.; Wang, Y.; Zhang, Z.; Tsang, H.K.; Lau, K.M. High-performance III-V photodetectors on a monolithic InP/SOI platform. Optica 2021, 8, 1204–1209.

43. Runge, P.; Zhou, G.; Ganzer, F.; Mutschall, S.; Seeger, A. Waveguide integrated InP-based photodetector for 100Gbaud applications operating at wavelengths of 1310nm and 1550nm. In Proceedings of the 2015 European Conference on Optical Communication (ECOC), Valencia, Spain, 27 September–1 October 2015; pp. 1–3.

44. Salamin, Y.; Ma, P.; Baeuerle, B.; Emboras, A.; Fedoryshyn, Y.; Heni, W.; Cheng, B.; Josten, A.; Leuthold, J. 100 GHz Plasmonic Photodetector. ACS Photonics 2018, 5, 3291–3297.